

Engineering of multicolor spatial solitons with chirped-period quasi-phase-matching gratings in optical parametric amplification

Andrew M. Schober and Martin M. Fejer

E. L. Ginzton Laboratory, Stanford University, Stanford, California 94305

Silvia Carrasco

*Department of Electrical & Computer Engineering and Department of Physics, Boston University,
Boston, Massachusetts 02215*

Lluís Torner

ICFO–Institut de Ciències Fotoniques, and Universitat Politècnica de Catalunya, Barcelona 08034, Spain

Received March 7, 2005

We demonstrate the excitation of solitons in a parametric amplifier with enhanced signal content through the use of a chirped-period quasi-phase-matching grating. This technique affords a low soliton threshold at the input end of a parametric amplifier, and the subsequent transformation to a desired soliton that exists at nonzero wave-vector mismatch through the use of a linearly chirped quasi-phase-matching grating. This approach has an advantage over direct excitation of solitons at nonzero wave-vector mismatch in uniform nonlinear materials and holds potential for improving the efficiency and mode quality of high-gain parametric amplifiers. © 2005 Optical Society of America

OCIS codes: 190.5530, 190.4410.

Optical parametric amplification (OPA) offers several advantages compared with conventional laser amplification: there is no inherent thermal loading that poses engineering challenges in the design of laser amplifiers; the frequency and bandwidth are not constrained by quantum transitions inside the amplifier medium, making OPA suitable for the amplification over a broad tuning range; and OPA is capable of extremely large gain, in excess of 100 dB, eliminating the need for regenerative amplifiers in the chirped-pulse amplification of ultrashort pulses. With a time-dependent pump, OPA can also eliminate the amplification of satellite pulses present in ultrafast laser amplifiers.

Although a plane-wave pump can be driven to complete depletion¹ (100% conversion to signal–idler pairs), it is difficult to achieve total conversion in optical parametric chirped-pulse amplification (OPCPA) with Gaussian beams (or otherwise spatially nonuniform beams). High photon conversion efficiency (58%) has been achieved through spatial and temporal flattening of the pump intensity²; however, lower photon conversion efficiency ($\leq 10\%$) is typical when using commercially available pump sources,³ and efficiency as high as 38% when the pump beam has a super-Gaussian spatial intensity envelope has been reported.⁴

Quasi-phase-matching (QPM) engineering allows tailoring the properties of parametric amplification, including the regime of quadratic soliton generation where the signal, idler, and pump waves propagate mutually trapped and locked together with high-quality beam modes (for a review of quadratic solitons, see Ref. 5). The tunability afforded by QPM allows engineering the soliton launching efficiency and

the soliton properties.^{6,7} The same idea holds for inhomogeneous phase matching induced, e.g., by temperature gradients.⁸ Generating solitons in a parametric amplifier and exploiting the properties of solitons subject to a changing local wave-vector mismatch in a chirped QPM grating was shown theoretically to allow increased conversion efficiency.⁹ Continuous-wave (CW) numerical simulations indicate that photon conversion efficiencies of 90% are possible with this technique. Moreover, it was shown to be relatively insensitive to changes in pump power and signal frequency, making it applicable to the amplification of short pulses in a chirped-pulse OPA. Generation of quadratic solitons in parametric amplification and parametric generation has been demonstrated,^{10,11} and high gain in an OPCPA system under conditions suitable for soliton formation featuring a photon conversion efficiency of 46% has been observed.¹² In this Letter, we demonstrate the manipulation of soliton properties through OPA in a chirped QPM grating in periodically poled lithium niobate (PPLN) and show the essential features of the efficiency-enhanced parametric amplifier put forward in Ref. 9.

The concept of chirped-grating soliton parametric amplification is illustrated in Fig. 1. The distribution of power among the signal, idler, and pump waves in a soliton is a function of wave-vector mismatch, defined as $\Delta k = k_1 + k_2 - k_3 + K_g$, where k_i is the wave vector for the signal ($i=1$), idler ($i=2$), or pump ($i=3$) wave, and $K_g = 2\pi/\Lambda$ is the grating vector of a QPM grating defined in terms of the QPM period Λ . The condition desirable for maximum conversion to signal–idler pairs in a soliton occurs when $\Delta k \gg 0$; however, the condition for low soliton excitation

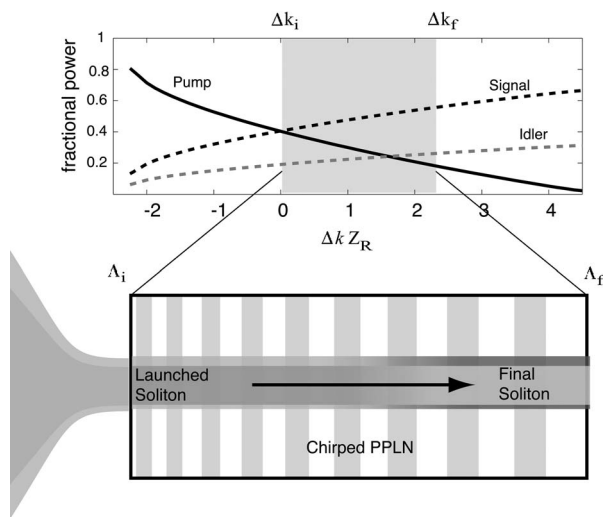


Fig. 1. Soliton parametric amplification with chirped gratings. The graph shows the power sharing between the component waves of an exact multicolor soliton as a function of wave-vector mismatch, normalized to the pump beam diffraction length Z_R ($Z_R=5.1$ mm in our experiment), for a soliton with 6 kW of total power. The bottom schematic shows how these properties can be mapped onto a chirped QPM grating.

threshold is $\Delta k \approx 0$, and the highest launching efficiency in OPA occurs at slightly negative Δk .¹³ A chirped QPM grating allows for $\Delta k \approx 0$ at the incident face of the nonlinear crystal for large launching efficiency and a smooth transformation to solitons at $\Delta k \gg 0$ at the end for maximum conversion efficiency.

The pump laser in our experiment is a JDS Uniphase PowerChip laser, a passively Q -switched Nd:YAG microchip laser that supplies 500-ps-long pump pulses with up to 50 μJ energy at a repetition rate of 1 kHz and a wavelength of 1064 nm. The CW signal is at a wavelength of 1553 nm with approximately 3 mW of output power. The pump and signal beams are combined using a dichroic mirror and focused to a spot size ($1/e^2$ diameter) of 55 μm at the input face of a 5-cm-long PPLN crystal. The 5-cm-long PPLN crystal used in this experiment is ten times longer than the diffraction length for a 55- μm -wide Gaussian beam. The pump beam in this experiment was measured to have a beam quality factor $M^2=1.5$, indicating faster divergence than the equivalent-width Gaussian TEM₀₀ beam.

The output light is separated by a second dichroic mirror into signal and pump beams. The exit face of the PPLN crystal is imaged using CCD cameras, a silicon camera for the pump and an InGaAs camera for the signal. The energies of the pump and signal waves were also measured using integrating photoreceivers that were time gated to reject energy in the unamplified CW signal that is present between pump pulses. No measurements were made on the idler wave.

In Fig. 2, we compare the soliton measured in a uniform grating at $\Delta k=0$ to the soliton obtained in a QPM grating chirped to a final mismatch $\Delta k_f=875$ m^{-1} . The soliton at the output of the chirped

grating has most of its energy in the signal (and idler) wave with reduced pump intensity compared with the uniform grating. Fringes are observed on the background of the image as a result of total internal reflection of nonsoliton fields at the surface of our 0.5-mm-thick PPLN samples.

To quantify the behavior for several chirped gratings, it was necessary to distinguish the soliton content in the output beam from unguided pump and signal light. Using the CCD images of the pump and signal spatial modes, we defined a circular digital mask centered at the peak of the soliton mode, and with a radius approximately twice the soliton radius. The sum of all pixel values inside this soliton radius divided by the sum of all pixels in the image is equal to the soliton energy divided by the total energy, and this ratio can be used with the measured total energy to calculate the soliton content. We measured the soliton energy in the pump and signal waves in several chirped gratings, all with initial mismatch $\Delta k_i=0$ (QPM period $\Lambda_i=29.56$ μm) and final wave-vector mismatch ranging from $\Delta k_f=-1000$ m^{-1} ($\Lambda_f=29.70$ μm) to $\Delta k_f=1000$ m^{-1} ($\Lambda_f=29.44$ μm).

The pump energy required to launch a soliton was 23–25 μJ . At this pump power, we observed soliton energies of 2–6 μJ , resulting in a launching efficiency of 8–26% near the soliton threshold for $\Delta k=0$. Numerical simulations for ideal pulse and beam quality conditions predict a launch efficiency in excess of 50%. The soliton energy at threshold is consistent with the numerical simulations, but the observed pump power required to excite solitons is thus higher than expected. This difference is attributed to the poor beam quality in our experiment. This is qualitatively consistent with simulations when the beam quality was spoiled through the addition of higher-order Laguerre–Gaussian modes. It is also consistent with recent measurements where the soliton threshold was observed to increase substantially with M^2 .¹⁴

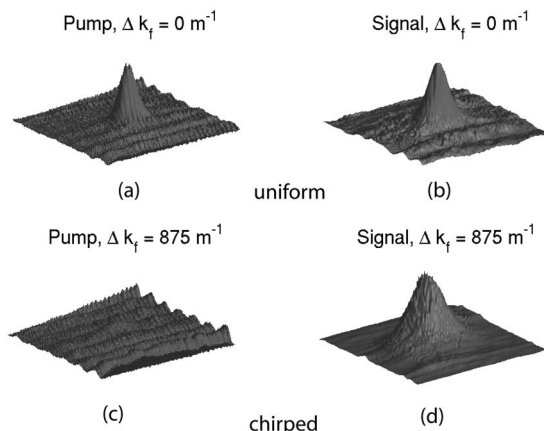


Fig. 2. Engineered solitons. Top row: surface plots show spatial intensity profile of (a) pump and (b) signal components of a multicolor soliton in a uniform grating at $\Delta k=0$. Bottom row: surface plots of pump (c) and signal (d) waves at the output of a chirped grating with initial wave-vector mismatch $\Delta k_i=0$ and final mismatch $\Delta k_f=875$ m^{-1} . Note the clearly higher conversion efficiency in the chirped grating case.

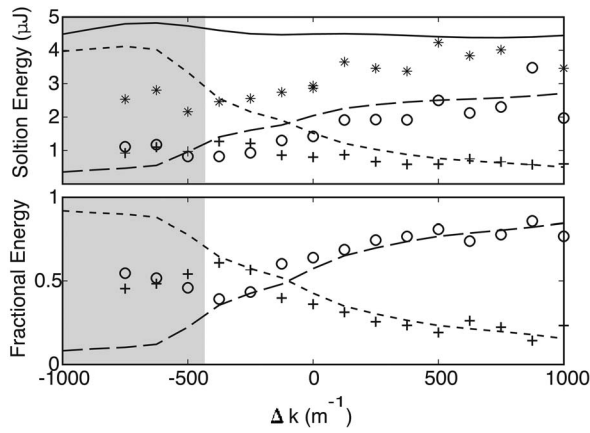


Fig. 3. Properties of engineered solitons. Top, energy inside a digital aperture of two input beam radii carried by the pump (crosses, experiment; short-dashed curve, simulation), signal (circles, experiment; dashed curve, simulation), and total (asterisks, experiment; solid curve, simulation) in chirped gratings versus final wave-vector mismatch. The initial mismatch in all cases is $\Delta k=0$. Bottom, fractional energy, defined as the signal or pump energy divided by the sum (signal+pump) energy. The shaded region indicates the presence of amplified vacuum noise. In that region the input peak power is below the soliton threshold, and thus solitons do not form.

The central result of our experiments is shown in Fig. 3. For comparison, we also plot results of numerical simulations conducted with CW evolution equations [see Eq. (1) of Ref. 9], assuming radial symmetry. The temporal shape of the pump pulse was included by averaging the results of CW propagations over a Gaussian temporal envelope. The conditions mimic the experimental conditions, except that the numerical simulations use a Gaussian pump field with energy of $8 \mu\text{J}$ to yield the same soliton energy as in the experiment.

The experimental data show reasonable agreement with simulations in the unshaded region. No solitons can form in the shaded region, since the energy is below the threshold. Parametric amplification of vacuum noise was observed in this region near the 1562-nm wavelength, far from the signal seed wavelength of 1553 nm and closer to the phase-matching wavelength for the final periods found in this region of the graph. Amplification of vacuum noise was not included in the numerical model, and this is the reason for the apparent disagreement between experiment and numerical simulation in the shaded portion of the graph. The spectral width of the signal in the unshaded region was measured to be less than 0.1 nm (the limit of our spectrometer) for all gratings.

In addition to the chirped grating experiments, we performed experiments in uniform gratings away from wave-vector matching that demonstrate a soli-

ton threshold that increases sharply with mismatch (positive or negative), and parametric generation is observed for $\Delta k < -125 \text{ m}^{-1}$ and $\Delta k > 750 \text{ m}^{-1}$. Optical damage was observed in some cases at the maximum available pump energy around $40 \mu\text{J}$ before the soliton threshold was reached in gratings with $|\Delta k| > 500 \text{ m}^{-1}$. This behavior demonstrates the clear advantage of launching solitons at $\Delta k=0$ and using a chirped QPM grating to access soliton states at large $|\Delta k|$, where it is difficult to achieve direct excitation in a high-gain parametric amplifier.

In conclusion, we have demonstrated engineering of solitons in OPA through the use of a chirped QPM grating, generating solitons near phase matching, where the launching soliton efficiency is close to optimum, and using a linearly chirped QPM grating to transform the energy sharing of the soliton to a more favorable value determined by the local wave-vector mismatch. This behavior demonstrates the essential features of an efficiency-enhanced soliton optical parametric amplifier.

A. M. Schober's e-mail address is schober@stanford.edu.

References

1. R. A. Baumgartner and R. L. Byer, *IEEE J. Quantum Electron.* **15**, 432 (1979).
2. L. J. Waxer, V. Bagnoud, I. A. Begishev, M. J. Guardalben, J. Puth, and J. D. Zuegel, *Opt. Lett.* **28**, 1245 (2003).
3. I. Jovanovic, C. Ebberts, and C. P. J. Barty, *Opt. Lett.* **27**, 1622 (2002).
4. I. Jovanovic, B. J. Comaskey, C. A. Ebberts, R. A. Bonner, D. M. Pennington, and E. C. Morse, *Appl. Opt.* **41**, 2923 (2002).
5. A. V. Buryak, P. D. Trapani, D. V. Skryabin, and S. Trillo, *Phys. Rep.* **370**, 63 (2002).
6. L. Torner, C. B. Clausen, and M. M. Fejer, *Opt. Lett.* **23**, 903 (1998).
7. S. Carrasco, J. P. Torres, L. Torner, and R. Schiek, *Opt. Lett.* **25**, 1273 (2000).
8. R. Schiek, R. Iwanow, T. Pertsch, G. I. Stegeman, G. Schreiber, and W. Sohler, *Opt. Lett.* **29**, 596 (2004).
9. S. Carrasco-Rodriguez, J. P. Torres, L. Torner, and M. M. Fejer, *J. Opt. Soc. Am. B* **19**, 1396 (2002).
10. M. T. G. Canva, R. A. Fuerst, S. Babiou, G. I. Stegeman, and G. Assanto, *Opt. Lett.* **22**, 1683 (1997).
11. P. DiTrapani, G. Valiulis, W. Chinaglia, and A. Andreoni, *Phys. Rev. Lett.* **80**, 265 (1998).
12. A. Galvanauskas, A. Hariharan, F. Raksi, K. K. Wong, D. Harter, G. Imeshev, and M. M. Fejer, in *Conference on Lasers and Electro-Optics*, Vol. 39 of OSA Trends in Optics and Photonics Series (Optical Society of America, 2000), paper CThB4.
13. S. Carrasco, L. Torner, J. P. Torres, D. Artigas, E. Lopez-Lago, V. Couderc, and A. Barthelemy, *IEEE J. Sel. Top. Quantum Electron.* **8**, 497 (2002).
14. H. Kim, L. Jankovic, G. Stegeman, S. Carrasco, L. Torner, D. Eger, and M. Katz, *Opt. Lett.* **28**, 640 (2003).